Food ingredient recognition model via image and textual feature extraction and hybrid classification strategy

Sharanabasappa A. Madival, Shivkumar S. Jawaligi

Food ingredient recognition model via image and textual feature extraction and hybrid classification strategy

Sharanabasappa A. Madival*

Department of Computer Science and Engineering,
Faculty of Engineering and Technology,
Sharnbasva University, India
Email: maddi.227@gmail.com
*Corresponding author

Shivkumar S. Jawaligi

Department of Electronic and Communication Engineering,
Faculty of Engineering and Technology,
Sharnbasva University,
Kalburgi, Karanataka, India
Email: shiv.jawaligi@gmail.com

Abstract: This research work focuses on food recognition, especially, the identification of the ingredients from food images. Here, the developed model includes two stages namely: 1) feature extraction; 2) classification. Initially, the image features and textual features will be extracted, where image features like SIFT and improved CNN-based deep features, textural features are extracted. Then, the hybrid classifier is used for the identification of food ingredients that combines the models like neural network (NN) as well as long short-term memory (LSTM). In order to make the accurate results, the weights of NN and LSTM are fine-tuned via the Chebyshev map evaluated teamwork optimisation (CME-TWO) algorithm. At the final stage, the primacy of the offered scheme is proven concerning varied metrics.

Keywords: food ingredients; improved CNN; TF-IDF features; long short-term memory; LSTM; CME-TWO algorithm.

Biographical notes: Sharanabasappa A. Madival is Associate Professor and the Chairman Department of Computer Science and Engineering at Sharnbasva University Kalaburagi, Karnataka, India. He has completed his MTech in Computer science and Engineering from Visvesvaraya Technological University, Belagavi. He has more than 20 years of teaching and research experience. His area of research is image processing. He has published more than eight research articles in international and national journals.

Shivkumar S. Jawaligi is presently working as a Professor and Dean, Faculty of Engineering and Technology, Sharnbasva University Kalaburagi, Karnataka, India. He has received his PhD from Visvesvaraya Technological University, Belagavi. He has more than 20 years of teaching and research experience. His area of specialisation is wireless sensor and image processing. He as published more than 25 research articles in international and national journals.

This paper is a revised and expanded version of a paper entitled 'A comprehensive review and open issues on food image analysis and dietary assessment', presented at 3rd International Conference on Intelligent Sustainable Systems (ICISS), Thoothukudi, India, 3–5 December 2020.

1   Introduction

The quantification and determination of food ingredients is a significant issue in authorised food management. The intricacy of foodstuffs, globalisation of grocery markets and complications in the traceability of trade channels unlocks the door for failures and fraud in the processing, stocking and labelling process (Aguiar et al., 2018; Liu et al., 2016; Zhao et al., 2020a). The feasible consequence for customers is diverse beginning with observance of moral aspects like vegan, kosher or halal over healthy risks formed by pathogenic creatures to uncomplicated frauds owing to

economical causes. Actually, organic pollutants made up the vast amount of forewarning notices released by German authorities in 2011 and 2015. Meat and its related commodities are among the food products, which are most susceptible to corruption owing to their comparatively higher value and demands in the marketplace (Macheka et al., 2021; Pearce et al., 2020; Hellmann et al., 2020).

Most of such cases were motivated by microbiological pollutants or the existence of non-declared allergic food elements (Liu et al., 2018; Li et al., 2020). As a result, drug and food legislation requires the appropriate assertion of ingredients and observance to transport and storage conditions (Lo et al., 2020; Liu et al., 2020). To guarantee observance to law and to sustain customer security, there is a rising requirement for schemes that permit for accurate determination of food elements, preferably straddling every kingdom of life together with fungi, plants bacteria, animals and maybe also expanding to viruses (Navruz-Varlı et al., 2018; Pang et al., 2020; Hellmann et al., 2020).

A broader palette of systematic techniques for examining products was introduced and is regularly deployed at authorised food control lab, however also industrial and private controlling labs (Iqbal et al., 2021; Fernandes et al., 2019; Wang et al., 2018a). Amongst these, DNA-oriented schemes such as PCR are perhaps the most extensively deployed methods, due to of their higher sensitivity and the prospect to carry out quantitative measures (Santosh Kumar and Venkata Ramanaiah, 2019; Nipanikar and Hima Deepthi, 2019; Vinusha, 2019; Sreenivasu et al., 2022). Nevertheless, while multiplexed or done in the meta bar coding arrangement, PCR-oriented schemes include the disadvantage to identify only a partial range of targeted classes and generate assay-based intensification bias (Wang et al., 2018b; Ambrosini et al., 2018; Wahls et al., 2014; Hellmann et al., 2020).

The contributions of the work are as follows:

- Introduces a new food ingredient recognition model, in which SIFT, improved CNN-based deep features, BOW and TF-IDF features.

- Exploits hybrid classifiers like neural network (NN) and long short-term memory (LSTM) for recognising purpose.

- Proposing a new algorithm termed as Chebyshev map evaluated team work optimisation (CME-TWO) for tuning the weights of LSTM and NN.

The paper is arranged as: Section 2 and Section 3 depict the reviews and extraction of features. Section 4 portrays CME-TWO-based optimised hybrid classifiers: NN + LSTM. Further, Section 5 addresses the steps followed in the proposed model. The results are briefed in Section 6 and the conclusions are described in Section 7.

2 Literature review

2.1 Related works

In 2018, Kuo et al. developed a technique for detecting the components of mullet roe stuff. Depending upon the 'TaqMan real-time PCR assay', specified mullets were designed, which targeted the RNA gene. Further, PCR amplicon was deployed for identifying fish variety in roe products slighter than 200 bp.

In 2020, Hellmann et al. analysed 'regional Doner kebap samples' that exposed unlabelled and unexpected plant and poultry elements in 3 of 5 cases. Additionally, AFS was systematically applied to a broader set of meat substances of well-known composition for evaluating probable limits and quantification accurateness. Also, a consequence of diverse food matrices was analysed in detail. The newly developed method performed far better and was remarkably accurate in the earlier studies.

In 2021, Zheng et al. screened six compounds from a natural product dataset through a cross-study depending upon two semi-flexible molecular dock techniques. It was shown that four elements have efficiently reduced thrombin and Calceolarioside B was most economical depending upon enzyme inhibiting experimentation. In addition, the required free energies of these elements with thrombin exhibited a steady rank tendency. The investigational results have shown the enhancement of this technique.

In 2020b, Zhao et al. developed a species-specified PCR united with LFI for the recognition of goose meat. The goose-specified primer, which particularly enriched a portion on the 'mitochondrial 12s RNA gene' were effectively modelled. The primer's specificity was confirmed in opposition to other species related to meat fraud. The simulated results have shown that the developed technique detected goose in cooked and uncooked binary mixtures.

In 2020, Hafiz et al. suggested a novel system to monitor the nutritional data on soft drinks via a DCNN approach. At first, pre-processing was done by means of noise minimisation as well as contrast enhancement. At last, the performances of the suggested method were confirmed regarding accuracy.

In 2020, Jiang et al. established a stage model for identifying food images by recognising the candidate locations and by deploying DCNN to classify the objects. In the beginning, RPN was deployed to generate several areas of proposals. Eventually, the dietary ingredients were examined based on detected outcomes as well as dietary evaluation was produced consequently.

In 2018, Emmanuel and Minija suggested a dietary valuation scheme depending on 'CSWWLIFC'. Initially, segmentation was done over the images depending on the conservative WLI-FC model. Besides, feature vectors were derived and trained by means of the WLM scheme. Finally, the accuracy of the suggested model was proved by carrying out tests using the executed model.

Table 1   Review on existing food ingredient recognition models

Author	Method	Features	Challenges
Kuo et al. (2018)	PCR	• High Specificity • Improved sensitivity	• Can be applied only for speedy screening purpose
Hellmann et al. (2020)	Read mapping	• Minimises false positive • High accuracy	• Screening power is limited till 20–30 species
Zheng et al. (2021)	Virtual screening	• Higher throughput screening • High accuracy	• Future works is on the concern on less toxicity foods
Zhao et al. (2020b)	PCR	• High sensitivity • Reduced cost	• Cost factors should be explored
Rubaiya et al. (Hafiz et al., 2020)	DCNN	• High throughput • Highly accurate	• Bottle size assessment is required
Jiang et al. (2020)	DCNN	• High accuracy • Better efficacy	• High processing time
Emmanuel and Minija (2018)	CSW-WLIFC	• Minimal error • Improved reliability	• Need analysis on cost
Wald et al. (2019)	Pearson correlation	• Improved data • Quality • Real time analysis	• Need to analyse market prices

In 2019, Wald et al. illustrated the appliance and substantiation of the CIMI scheme in a Ghanaian country. The elementary structure of CIMI was designed by arranging a questionnaire on the rate of recurrence of food and as a result, region-oriented food groups were recognised via food composition tables. In addition, substantiation was done by means of a correlation study.

2.2   *Review*

Table 1 shows the reviews on secured TS systems. Initially, PCR was deployed in Kuo et al. (2018) which offered specificity and it also improved sensitivity. Nevertheless, it can be applied only for speedy screening purposes. Read mapping was exploited in Hellmann et al. (2020) that offered higher accuracy with minimal false positives; however, screening power is limited to 20–30 species. In addition, virtual screening was introduced in Zheng et al. (2021), which increased throughput screening along with high accuracy. Nevertheless, future work is on the concern of fewer toxicity foods. Likewise, PCR model was exploited in Zhao et al. (2020b), that minimised cost and it is offered high sensitivity. However, cost factors should be explored. Moreover, the DCNN model was deployed in Hafiz et al. (2020), which offered high accuracy and it included high throughput; however, bottle size assessment is required. DCNN was exploited in Jiang et al. (2020) that offer high accuracy and better efficacy however, it incurs high processing time. CSW-WLIFC was suggested in Emmanuel and Minija (2018) with higher reliability and it also presented minimal error. However, it needs analysis on cost. Finally, Pearson correlation was implemented in Wald et al. (2019), which offered improved data quality and it provided

real-time analysis, however it needs to analyse market prices.

3   Extraction of features for developed food ingredient recognition model

The initial process is about extracting features like:

1   SIFT

2   improved CNN-based deep features

3   BOW features

4   TF-IDF features.

3.1   *SIFT features*

The SIFT (SIFT Feature, https://medium.com/data-breach/introduction-to-sift-scaleinvariant-feature-transform-65d7f3a72d40) is a simpler process and it encompasses four phases:

a   Electing scale-space peak: A probable spot to locate features is elected from the input image. The scale shape is computed as in equation (1), in which, $\text{Im}_{(c,d)}$ implies a segmented image with pixels (c, d) and $G_{(c,d,\sigma)}$ denotes Gaussian variable scale.

$$L_{(c,d,\sigma)} = G_{(c,d,\sigma)} * \text{Im}_{(c,d)} \tag{1}$$

In addition, $*$ implies a convolution operator. The diverse strategies are employed to find the positions of constant key point. DoG helps to locate scale-space extrema, $K_{(c,d,\sigma)}$ by computing the difference amongst two images, one with scale l times over the other.

$$K_{(c,d,\sigma)} = O_{(c,d,l,\sigma)} - O_{(c,d,\sigma)} \qquad (2)$$

b Localisation of key points: The feature key points are located precisely from the selected scale-space peak. The extrema location Q is according to equation (3).

$$Q = \frac{\partial^2 K^{-1}}{\partial c^2} \frac{\partial^2 K}{\partial c} \qquad (3)$$

c Allotting orientation to key points: A scale-based neighbourhood is drawn around the key point site, and the gradient's size and direction are noted. The final product is a 3,600 orientation histogram with 36 bins. The histogram is produced as a result. The histogram will max out at different times. The orientation ϕ is computed as in equation (4).

$$\phi_{(c,d)} = \tan\left(O_{(c,d+1)} - O_{(c,d-1)} / O_{(c+1,d)} - O_{(c-1,y)}\right) \qquad (4)$$

d Key point descriptor: The key points are represented by a high-dimensional vector. An orientation, size, and position are included for each important point. The next step is to develop a description that is substantially distinctive for the local image area of each key point.

e Key point matching: The closest neighbours of the two images' key points are identified and paired.

The SIFT feature, which has been extracted is signified as FT^{SIFT}.

3.2 Improved CNN-based deep features

CNN (Gu et al., 2018) includes three varied layers:

- convolution layer
- pooling layer
- fully connected layer.

All neurons are linked with nearby neurons in the previous layer. At the position (r, t) in lth layer of the linked wth feature map, the features are evaluated as in equation (5).

$$B_{r,t,w}^l = W_w^{lT} PI_{r,t}^l + D_w^l \qquad (5)$$

In equation (5), W_w^l signifies weight, D_w^l signifies bias of wth filter linked to lth layer. At centre location (r, t) of lth layer, the patch input is denoted by $PI_{r,t}^l$. The activation value $(act_{r,t,w}^l)$ linked with existing features $B_{r,t,w}^l$ is assessed as presented in equation (6). In this work, leaky Relu function is used as activation function.

$$act_{r,t,w}^l = act\left(B_{r,t,w}^l\right) \qquad (6)$$

Pooling layer: In the poling layer, the downsampling function is carried out. For every pooling function $pool(\cdot)$ linked to $act_{m,h,w}^l$, the $C_{r,t,w}^l$ value is assessed as exposed in equation (7), in which, $NN_{r,t}$ signifies neighbours near a location (r, t).

$$C_{r,t,w}^l = pool\left(act_{m,h,w}^l\right), \forall (m, h) \in NN_{r,t} \qquad (7)$$

The results of prediction occur at CNN's output layer. The CNN loss is indicated as L and traditionally, it is exposed as in equation (8). Based on the proposed concept, CNN loss is calculated as given in equation (9).

$$L = \frac{1}{wn} \sum_{h=1}^{wn} l\left(\theta; C^{(h)}, F^{(h)}\right) \qquad (8)$$

$Loss =$

$$-\left[\prod_{n=1}^{N}\left(F^{(h)} - \log\left(C^{(h)}\right) - \left(1 - F^{(h)}\right)\right)\log\left(1 - C^{(h)}\right)\right]^{\frac{1}{N}} \qquad (9)$$

The general constraint correlated with W_w^l and D_w^l is denoted by θ. Thus, wn counts of output-input relation exist $\{(PI^{(h)}, C^{(h)}); h \in [1, \cdots, wn]\}$. The hth input feature, output as well as target labels are given by $PI^{(h)}$, $C^{(h)}$ and $F^{(h)}$, correspondingly. Here, the geometric mean function is deployed for computing the average entropy value. The extracted improved CNN feature is denoted as FT^{ICNN}.

3.3 BOW features

The text is converted into a bag of words in BOW (Thulasi, 2017). The feature matrix is created with size $m \times n$. Here, m denotes the count of sentence in the corpus and the count of unique words is denoted by n. The BOW-oriented feature, which is derived are denoted as FT^{BOW}.

3.4 TF-IDF features

TF–IDF (Kim et al., 2018) is a significant format of text demonstration and includes longer history amongst three well-known depiction techniques. According to BOW technique, a text is defined by a collection of words used inside the document. The constraint TF_{ij} is signified as times word count i found in the document j the better the value, the more notable the word will be. The constraint DF_i indicates document count, in which word i appears once; the better the value, the more frequent the word is. If word i is significant for document j, it must comprise a superior TF_{ij} and lesser DF_i (Guo and Yang, 2016). Here, TF-IDF features are shown in equation (10), where, TF_{ij} denotes the times word count i appear in document j, M denotes count of document in collection, n_i denotes total count of documents, in which features appear.

$$f^{TF\text{-}IDF} = TF \times IDF_{ij} = \frac{TF_{ij} \times \log\left(\frac{M}{n_i} + 0.01\right)}{\sqrt{\sum_{i=1}^{M} TF_{ij} \times \log^2\left(\frac{M}{n_i} + 0.01\right)}} \qquad (10)$$

The extracted TF-IDF-based features are indicated as $FT^{TF\text{-}IDF}$.

Consequently, the derived SIFT, BOW, TF-IDF and improved CNN-based deep features are estimated as FT, i.e., $FT^{SIFT} + FT^{BOW} + FT^{TF\text{-}IDF} + FT^{ICNN} = FT$ that are then classified via HC for recognition.

4   CME-TWO-based optimised hybrid classifiers: NN + LSTM

4.1   Optimised NN classifier

It (Mohan et al., 2016) concerns on optimal features FT as input, as exposed in equation (11), wherein nu indicates whole count of features.

$$FT = \{FT_1, FT_2, \ldots\ldots, FT_{nu}\} \tag{11}$$

The NN scheme (Mohan et al., 2016) encompasses hidden, output and input layers. In equation (12), the hidden layer output $z^{(H)}$ is exposed and output of network $\hat{Q}_{\hat{o}}$ is described in equation (13). Here, $\hat{i}$ and $j \rightarrow$ neurons of input and hidden layers, $F \rightarrow$ activation functions, $We_{(B\hat{i})}^{(H)} \rightarrow$ bias weight to $\hat{i}^{\text{th}}$ hidden neuron, $n_{\hat{i}} \rightarrow$ input neurons count and $We_{(j\hat{i})}^{(H)}$ is the weight from j^{th} input neuron to $\hat{i}^{\text{th}}$ hidden neuron, $\hat{o}$ is the output neurons, n_h indicates the count of hidden neuron, $We_{(B\hat{o})}^{(P)} \rightarrow$ output bias weight to $\hat{o}^{\text{th}}$ output layer, and $We_{(\hat{i}\hat{o})}^{(P)} \rightarrow$ weight from $\hat{i}^{\text{th}}$ hidden layer to $\hat{o}^{\text{th}}$ output layer. The errors between predicted and actual values are specified in equation (14), wherein, $n_G \rightarrow$ output neuron count, $\hat{P}_{\hat{o}}$ and $P_{\hat{o}}$ is the output of predicted as well as actual value.

$$z^{(H)} = F\left(We_{(B\hat{i})}^{(H)} + \sum_{j=1}^{n_i} We_{(j\hat{i})}^{(H)} FT\right) \tag{12}$$

$$\hat{P}_{\hat{o}} = F\left(We_{(B\hat{o})}^{(P)} + \sum_{\hat{i}=1}^{n_h} We_{(\hat{i}\hat{o})}^{(P)} z^{(H)}\right) \tag{13}$$

$$Er^* = \underset{\left\{We_{(B\hat{i})}^{(H)}, We_{(j\hat{i})}^{(H)}, We_{(B\hat{o})}^{(P)}, We_{(\hat{i}\hat{o})}^{(P)}\right\}}{\arg\min} \sum_{=1}^{n_G} \left|P_{\hat{o}} - \hat{P}_{\hat{o}}\right| \tag{14}$$

The output from NN classifier offers the final classified output in a precise way.

Here, the weights of NN denoted by We are optimally elected by the proposed CME-TWO model.

4.2   Optimised LSTM classifier

It (Zhou et al., 2019) incorporates a sequence of recurring LSTM cells. Each cell of LSTM comprises three units, such as 'input gate, output gate and forget gate'. The variables M indicates hidden state and D cell state. (X_t, D_{t-1}, M_{t-1}) indicates input layers and (M_t, D_t) output layers.

The O_t, I_t, F_t indicates the output, input and forget gate in time t. LSTM mostly setup F_t for data sorting to be ignored. The sorted data designate specific partial features related to prior gaze direction; F_t is modelled as in equation (15).

$$F_t = \sigma\left(U_{IF}X_t + B_{IF} + U_{MF}M_{t-1} + B_{MF}\right) \tag{15}$$

In equation (15), (U_{IF}, B_{IF}) and (U_{MF}, B_{MF}) suggest bias and weight constraint to map hidden and input layers to forget gate as well as activation function is inferred by σ.

Input gate in LSTM as exposed in equation (16)–equation (18), in which, (U_{MG}, B_{MG}) and (U_{IG}, B_{IG}) signifies weight as well as bias constraint for mapping hidden and input layers to cell gate. (U_{MI}, B_{MI}) and (U_{II}, B_{II}) imply weight and bias constraint to map hidden and input layers to I_t.

$$G_t = \tanh\left(U_{IG}X_t + B_{IG} + U_{MG}M_{t-1} + B_{MG}\right) \tag{16}$$

$$I_t = \sigma\left(U_{II}X_t + B_{II} + U_{MI}M_{t-1} + B_{MI}\right) \tag{17}$$

$$D_t = F_t D_{t-1} + I_t G_t \tag{18}$$

$$O_t = \sigma\left(U_{IO}X_t + B_{IO} + U_{MO}M_{t-1} + B_{MO}\right) \tag{19}$$

$$M_t = O_t \tanh\left(D_t\right) \tag{20}$$

LSTM cell attains the output hidden layer from output gate as exposed in equation (19) and equation (20), where (U_{MO}, B_{MO}) and (U_{IO}, B_{IO}) implies weight a well as bias to map the hidden and input layer to O_t. Specifically, the weights of LSTM denoted by U are optimally elected by the new CME-TWO model.

4.3   Proposed CME-TWO model

- Objective: The objective Obj is to lessen the error as exposed in equation (21), in which, Err refers to error.

$$Obj = \min(Err) \tag{21}$$

- Solution encoding: The weights of NN (We) and LSTM weights indicated by (U) are chosen optimally via CME-TWO scheme. The representation of solutions is shown in Figure 1, wherein, wn and wm stand for the entire count of NN weights and LSTM weights.

Figure 1   Solution encoding (see online version for colours)
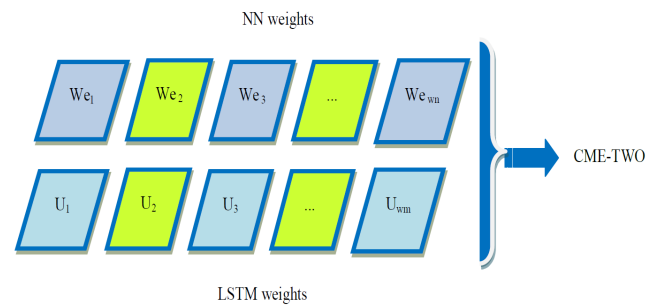
4.4   CME-TWO

CME-TWO is an enhanced edition of the benchmark TOA model. Existing TOA model addresses the collaboration behaviour of team members to achieve their planned aim. The TOA model is good in resolving the optimisation problems. Although, the TOA (Dehghani and Trojovský, 2021) is highly convergent, at certain times, it gets stuck within the local optima. Thus, the global best solutions

could not be accomplished. As a result, in this research work, the information sharing and individual activity phases of TOA are customised for enhancing the convergence speed. Normally, self-development is established to be capable to resolve countless multifaceted optimisation problems (Rajakumar, 2013a, 2013b; Swamy et al., 2013; George and Rajakumar, 2013; Rajakumar and George, 2012; https://neptune.ai/blog/gan-loss-functions; https://nextjournal.com/jbowles/n-gram-models-part-1#:~: text=An%20n%2Dgram%20model%20is,rich%20pattern% 20discovery%20in%20text.&text=In%20other%20words%2 C%20it%20tries,or%20words%20near%20each%20other; Wagh and Gomathi, 2019; Sadashiv Halbhavi et al., 2019; Jadhav and Gomathi, 2019. The steps followed in CME-TWO model are described below:

Step 1   The count of team members (*M*) and iterations *Max^{itr}* is set.

Step 2   Randomly generate the initial population matrix.

Step 3   The objective function is computed for all search agents as in equation (21).

Step 4   For *itr* = 1: *Max^{itr}* do

Step 5   Supervisor is updated as in equation (22).

Step 6   For *i* = 1: *M* do

a   Supervisory guidance: The initial phase is to update team members based upon supervisory directions. The supervisor now directs the remaining team members toward the best outcome by sharing their experience and reports with them. Equations (22) to (24) are used to update the search agent's position, where X_i^{S1} indicates team member's new status *i* under the supervisor guidance. By tradition, *ran* is believed as a random integer, however, as per CME-TWO model, *ran* is computed using Chebyshev map.

$$X_i^{S1}: x_{i,d}^{S1} = x_{i,d} + ran * (S_s - I * x_{i,d}) \quad (22)$$

$$X_i = \begin{cases} X_i^{S1} & Obj_i^{S1} < Obj_i \\ X_i & else \end{cases} \quad (23)$$

$$I = round(1 + rand) \quad (24)$$

From equation (23), Obj_i^{S1} signifies the objective function and $x_{i,d}^{S1}$ signifies new value of *i*th search agent for *d*th problem. From equation (24), *I* denotes the update index value and *rand* indicates the random value generated among [0, 1].

b   Information sharing: At subsequent stage, every team member seeks to develop their performance with the information of other better team members. The better team members are identified and further M_i is determined for *i*th team member. Conventionally, this update is undergone based on equation (25); nevertheless, as per developed CME-TWO model, the update occurs on the basis of harmonic mean as given in equation (26) and X_i is modelled as in equation (27) and equation (28).

$$X^{N,i}: x_d^{N,i} = \frac{\sum_{j=1}^{M_i} x_{j,d}^{g,i}}{M_i} \quad (25)$$

$$X^{N,i}: x_d^{N,i} = \frac{M_i}{\sum_{j=1}^{M_i} x_{j,d}^{g,i}} \quad (26)$$

$$x_i^{S2}: x_{i,d}^{S2} = x_{i,d} + ran * (x_d^{N,i} - I * x_d) \\ * sign(Obj_i - Obj^{N,i}) \quad (27)$$

$$X_i = \begin{cases} X_i^{S2} & Obj_i^{S2} < Obj_i \\ X_i & else \end{cases} \quad (28)$$

In equation (27), $X^{N,i}$ implies team member's mean value of that is better than team member *i*. Also, $Obj^{N,i}$ implies objective function and M_i implies count of team member that is higher than *i*th search agent and X_i^{S2} implies team member's new status.

c   Individual activity: At this stage, each team member makes an effort to improve their performance in light of their current situation. We have a part to perform even in this time period. As shown in equation (29) and equation (30) respectively, a novel mathematical model is developed, where X_i^{S3} implies third stage new status of team member and Obj_i^{S3} implies objective function.

$$x_i^{S3}: x_{i,d}^{S3} = x_{i,best} + (-0.01 + ran * 0.02) * x_{i,d} \quad (29)$$

$$X_i = \begin{cases} X_i^{S3} & Obj_i^{S3} < Obj_i \\ X_i & else \end{cases} \quad (30)$$

Step 7   End for *i* = 1: *M*, *itr* = 1: *Max^{itr}*.

Step 8   Save the attained best solution.

Step 9   End for *itr* = 1: *Max^{itr}*.

Step 10   Return best solution

Step 11   Terminate

5   Steps followed in proposed food ingredient identification model

The proposed model comprises three very important phases:

- Initially, SIFT, improved CNN-based deep features, BOW features and TF-IDF features are derived as features.

- Subsequently, hybrid classifier is used for the identification of food ingredients that combines the models like NN and LSTM.

- To make the identification more accurate, the weights of NN and LSTM are tuned optimally using CME-TWO model.

Figure 2 depicts the overall description of proposed CME-TWO model.

Figure 2   Illustrative revelation for developed food ingredient identification model (see online version for colours)
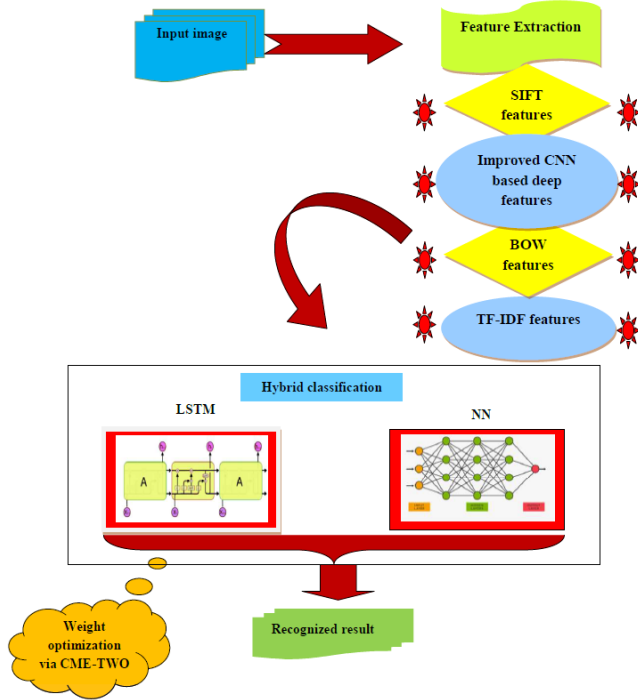
6   Results and discussion

6.1   Simulation procedure

The proposed HC + CME-TWO method for proposed scheme was executed in 'MATLAB' and the examination was done. Here, investigation was made by means of the dataset downloaded from http://www.ub.edu/cvub/ recipes5k/. The performance of developed scheme was computed over existing models such as HC + SA-CSO (Madival and Jawaligi, 2022), HC + PRO, HC + LA, HC + BFO, HC + SSO and HC + TWO regarding diverse metrics. In addition, examination was held amongst diverse classifiers like BI-LSTM, NN, LSTM, DBN and GRU.

Moreover, statistical analysis was performed to suggest the effectiveness of presented method.

6.2   Ingredient analysis

The targeted outputs and the actual outputs attained for six different food ingredients are illustrated in Table 2. The targeted outputs and the actual outputs are determined for varied schemes such as HC + SA-CSO (Madival and Jawaligi, 2022), HC + PRO, HC + LA, HC + BFO, HC + SSO and HC + TWO. From Table 2, it can be noticed that the output attained by developed CME-TWO model is almost similar to the targeted outputs.

6.3   Performance analysis

This section elaborates the performances of proposed HC + CME-TWO model over existing optimisation schemes concerning varied metrics. Here, evaluation was done using dataset from http://www.ub.edu/cvub/recipes5k/ and the related outcomes are graphed from Figures 3–5. The developed HC + CMETWO model is computed over HC + SA-CSO (Madival and Jawaligi, 2022), HC + PRO, HC + LA, HC + BFO, HC + SSO and HC + TWO models for varied LRs that ranges from 60, 70, 80 and 90. Moreover, Table 3 depicts the assessment of deployed scheme over conservative classifier schemes. In Figure 3, the proposed scheme has attained minimal negative outputs and increased positive outputs. Particularly, improved accuracy outputs are accomplished at 90th LR for proposed and existing schemes. Specifically, better accuracy values of (0.96) are attained for Figure 3(b), by proposed method at 60th LR, while, for other LPs, the accuracy values accomplished by developed model are relatively negligible. In addition, from Table 3, the HC + CME-TWO model concerning each metric has shown improved results for constructive metrics as well as minimal results for negative metrics with extant schemes. Therefore, the analysis shows the higher efficacy of HC + CME-TWO with the amalgamation of optimisation concept.

6.4   Convergence analysis

The convergence analysis of developed CME-TWO model with traditional models like, SACSO, LA, BFO, TWO, PRO and SSO for various iterations is illustrated in Figure 6. Here, the analysis is carried out by changing the iterations from 0, 5, 10, 15, 20, 25, 30 and 35. In general, the cost values of the proposed method have to be lesser for enhanced system performance. From Figure 6, the cost values are slightly better for proposed model from iteration 0 to 3, whereas, the adopted method shows least cost values than that of the cost values from iteration 4 to 35, accomplished in iteration 0 to 3. Here, conventional PRO and BFO models have showed worst performance than SA-CSO, LA, TWO and SSO ones. Thus, the overall assessment shows the superior performance of the proposed model.

Table 2 Sample image representation of anomaly localised frames in a video (see online version for colours)

Targeted output	{'Almond beets cheese dijon greens honey lemon oil onion pepper salt spinach vinaigrette vinegar'}	{'Berry egg flour milk oil salt shortening sugar warm water water yeast'}	{'Blueberries egg flour lemon milk oil salt shortening sugar vanilla warm water yeast'}	{'Apple beans beef carrot cauliflower coconut date egg garlic gin oil pepper rice salt scallions seeds shiitake spinach sriracha water zucchini'}	{'Beans beef brown sugar cloves egg gin kimchi oil pear reduced soy rice scallions'}	{'Bread cinnamon egg milk sugar vanilla'}
HC + CME-TWO	{'Almond beets cheese dijon greens honey lemon oil onion pepper salt spinach vinaigrette vinegar water'}	{'Berry egg flour milk oil salt shortening sugar'}	{'Blueberries egg flour lemon milk oil salt shortening sugar vanilla'}	{'Apple beans beef carrot cauliflower coconut date egg garlic gin oil pepper rice salt scallions seeds shiitake spinach sriracha worcestershire'}	{'Beans beef brown sugar cloves egg gin kimchi oil pear reduced soy rice scallions'}	{'Bread cinnamon egg milk sugar vanilla'}
HC + TWO	{'Almond beets cheese dijon greens honey lemon oil onion pepper salt spinach'}	{'Berry egg flour milk oil salt shortening sugar thyme tomato tuna vanilla vegemite vinegar vitamin water worcestershire xylitol sweetener zucchini'}	{'Blueberries egg flour lemon milk oil salt shortening sugar thyme tomato tuna vanilla vegemite vinegar vitamin water worcestershire xylitol sweetener zucchini'}	{'Apple beans beef carrot cauliflower coconut date egg garlic gin oil pepper rice salt scallions seeds shiitake spinach sriracha thyme tomato tuna vanilla vegemite vinegar vitamin water worcestershire xylitol sweetener zucchini'}	{'Beans beef brown sugar cloves egg gin kimchi oil pear reduced soy rice scallions thyme tomato tuna vanilla vegemite vinegar vitamin water worcestershire xylitol sweetener zucchini'}	{'Bread cinnamon egg milk sugar thyme tomato tuna vanilla vegemite vinegar vitamin water worcestershire xylitol sweetener zucchini'}
HC + SSO	{'Almond beets cheese dijon greens honey lemon oil onion pepper salt spinach'}	{'Berry egg flour milk oil salt shortening sugar vanilla vegemite vinegar vitamin wasabi water worcestershire xylitol sweetener yeast zucchini'}	{'Blueberries egg flour lemon milk oil salt shortening sugar vanilla vegemite vinegar vitamin wasabi water worcestershire xylitol sweetener yeast yolk zucchini'}	{'Apple beans beef carrot cauliflower coconut date egg garlic gin oil pepper rice salt scallions seeds shiitake spinach sriracha vanilla vegemite vinegar vitamin wasabi water worcestershire xylitol sweetener yeast yolk zucchini'}	{'Beans beef brown sugar cloves egg gin kimchi oil pear reduced soy rice scallions vanilla vegemite vinegar vitamin wafer wasabi water worcestershire xylitol sweetener yeast yolk zucchini'}	{'Bread cinnamon egg milk sugar vanilla vegemite vinegar vitamin wasabi water worcestershire xylitol sweetener yeast yolk zucchini'}
HC + LA	{'Almond beets cheese dijon greens honey lemon oil onion pepper salt'}	{'Berry egg flour milk oil salt seafood seeds shallot sherry shiitake sirloin soy spinach sugar tuna udon vanilla vitamin water xylitol sweetener yolk zucchini'}	{'Blueberries egg flour lemon milk oil salt seafood seeds shallot sherry shiitake sirloin soy spinach sugar tuna udon vanilla vitamin water yeast yolk zucchini'}	{'Apple beans beef carrot cauliflower coconut date egg garlic gin oil pepper rice salt scallions seafood seeds shallot sherry shiitake sirloin soy spinach sriracha tuna udon vanilla vitamin water yeast yolk zucchini'}	{'Beans beef brown sugar cloves egg gin kimchi oil pear reduced soy rice scallions seafood seeds shallot sherry shiitake sirloin soy spinach tuna udon vanilla vitamin water yeast yolk zucchini'}	{'Bread cinnamon egg milk seafood seeds shallot sherry shiitake sirloin soy spinach sugar tuna udon vanilla vitamin water yeast yolk zucchini'}

Note: (a) Image 1, (b) image 2, (c) image 3, (d) image 4, (e) image 5 and (f) image 5

Table 2   Sample image representation of anomaly localised frames in a video (continued) (see online version for colours)

	(a)	(b)	(c)	(d)	(e)	(f)
HC + PRO	{'Almond beets cheese dijon greens honey lemon oil onion pepper salt spinach vinaigrette vinegar'}	{'Berry egg flour milk oil salt shortening sugar tartar tenderloin Thai chilli toast tomato vanilla bean vanilla essence warm water yeast'}	{'Blueberries egg flour lemon milk oil salt shortening sugar tartar tenderloin Thai chilli toast tomato vanilla essence warm water yeast'}	{'Apple beans beef carrot cauliflower coconut date egg garlic gin oil pepper rice salt scallions seeds shiitake spinach sriracha tartar tenderloin Thai chilli toast tomato vanilla essence water zucchini'}	{'Beans beef brown sugar cloves egg gin kimchi oil pear reduced soy rice scallions tartar tenderloin Thai chilli toast tomato vanilla essence'}	{'Bread cinnamon egg milk sugar tartar tenderloin Thai chilli toast tomato vanilla essence'}
HC + BFO	{'Almond beets cheese dijon greens honey lemon oil onion pepper salt spinach vinaigrette vinegar'}	{'Berry egg flour milk oil salt shortening strip loin tenderloin Thai chilli thyme tofu warm water yeast'}	{'Blueberries egg flour lemon milk oil salt shortening strip loin tenderloin Thai chilli thyme tofu vanilla warm water yeast'}	{'Apple beans beef carrot cauliflower coconut date egg garlic gin oil pepper rice salt scallions seeds shiitake spinach sriracha strip loin tenderloin Thai chilli thyme tofu water zucchini'}	{'Beans beef brown sugar cloves egg gin kimchi oil pear reduced soy rice scallions strip loin tenderloin Thai chilli thyme tofu'}	{'Bread cinnamon egg milk strip loin tenderloin Thai chilli thyme tofu vanilla'}
HC + SACSO	{'Almond beets cheese dijon greens honey lemon oil onion pepper salt spinach vinaigrette vinegar'}	{'Berry egg flour milk oil salt shortening strip loin tenderloin Thai chilli thyme tofu warm water yeast'}	{'Blueberries egg flour lemon milk oil salt shortening strip loin tenderloin Thai chilli thyme tofu vanilla warm water yeast'}	{'Apple beans beef carrot cauliflower coconut date egg garlic gin oil pepper rice salt scallions seeds shiitake spinach sriracha strip loin tenderloin Thai chilli thyme tofu water zucchini'}	{'Beans beef brown sugar cloves egg gin kimchi oil pear reduced soy rice scallions strip loin tenderloin Thai chilli thyme tofu'}	{'Bread cinnamon egg milk strip loin tenderloin Thai chilli thyme tofu vanilla'}
	(a)	(b)	(c)	(d)	(e)	(f)

Note: (a) Image 1, (b) image 2, (c) image 3, (d) image 4, (e) image 5 and (f) image 5

Figure 3   Analysis on HC + CME-TWO with traditional optimisation method concerning (a) precision (b) accuracy (c) specificity and (d) sensitivity (see online version for colours)

(a)

(b)

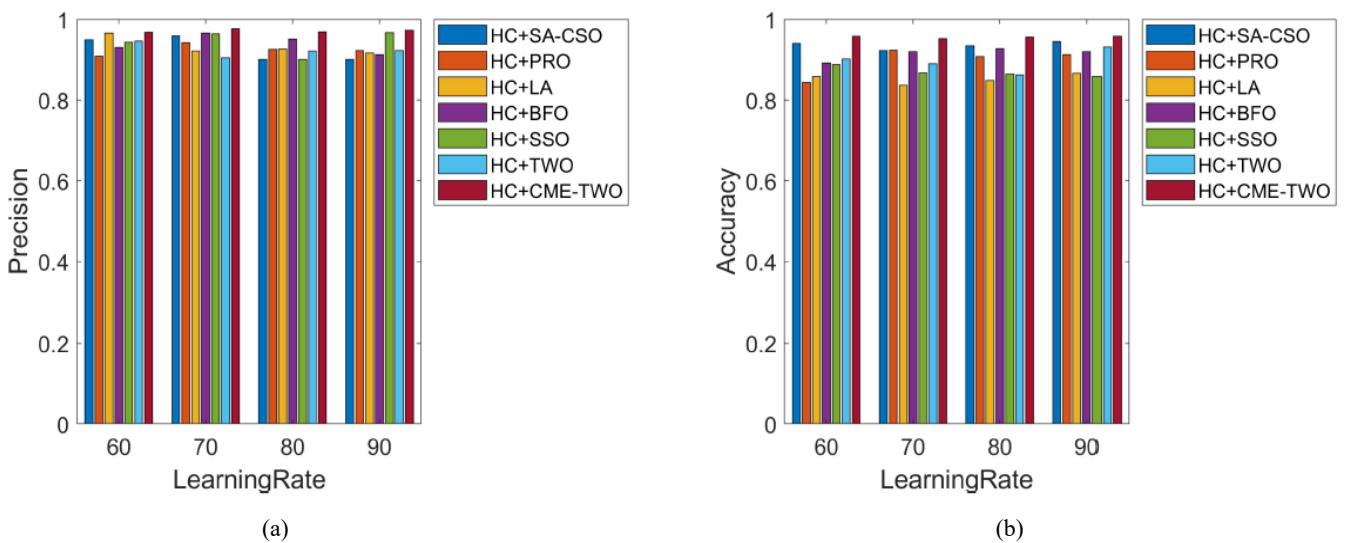**Figure 3** Analysis on HC + CME-TWO with traditional optimisation method concerning (a) precision (b) accuracy (c) specificity and (d) sensitivity (continued) (see online version for colours)
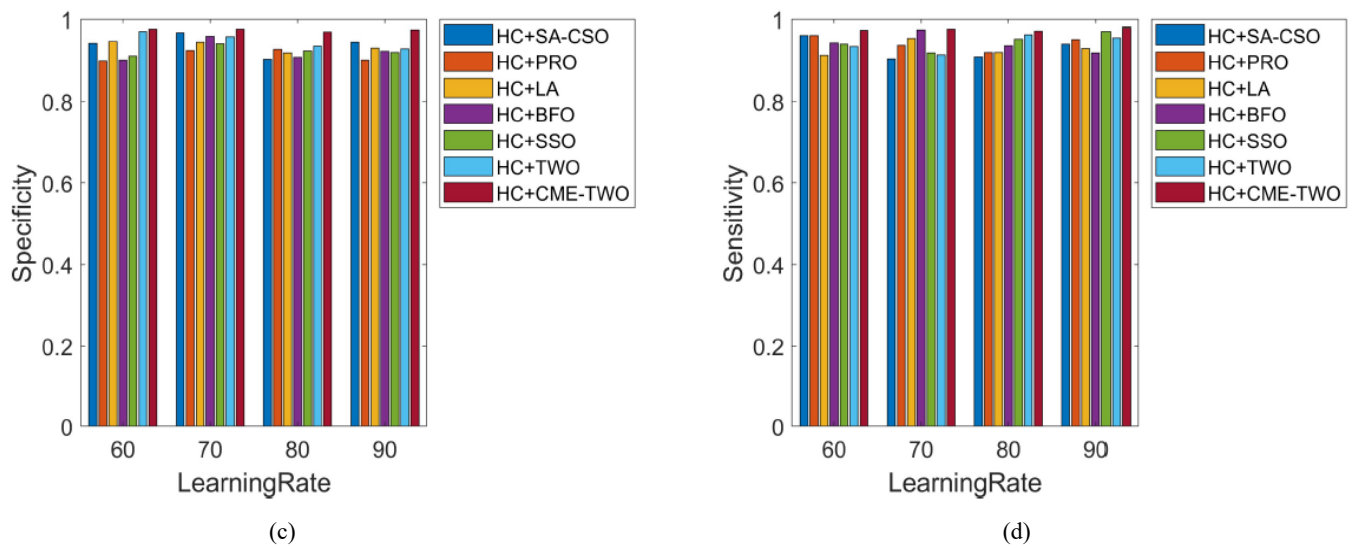

(c)

(d)

Figure 4 Analysis on HC + CME-TWO over traditional optimisation method concerning (a) MCC (b) NPV and (c) F1-score (see online version for colours)
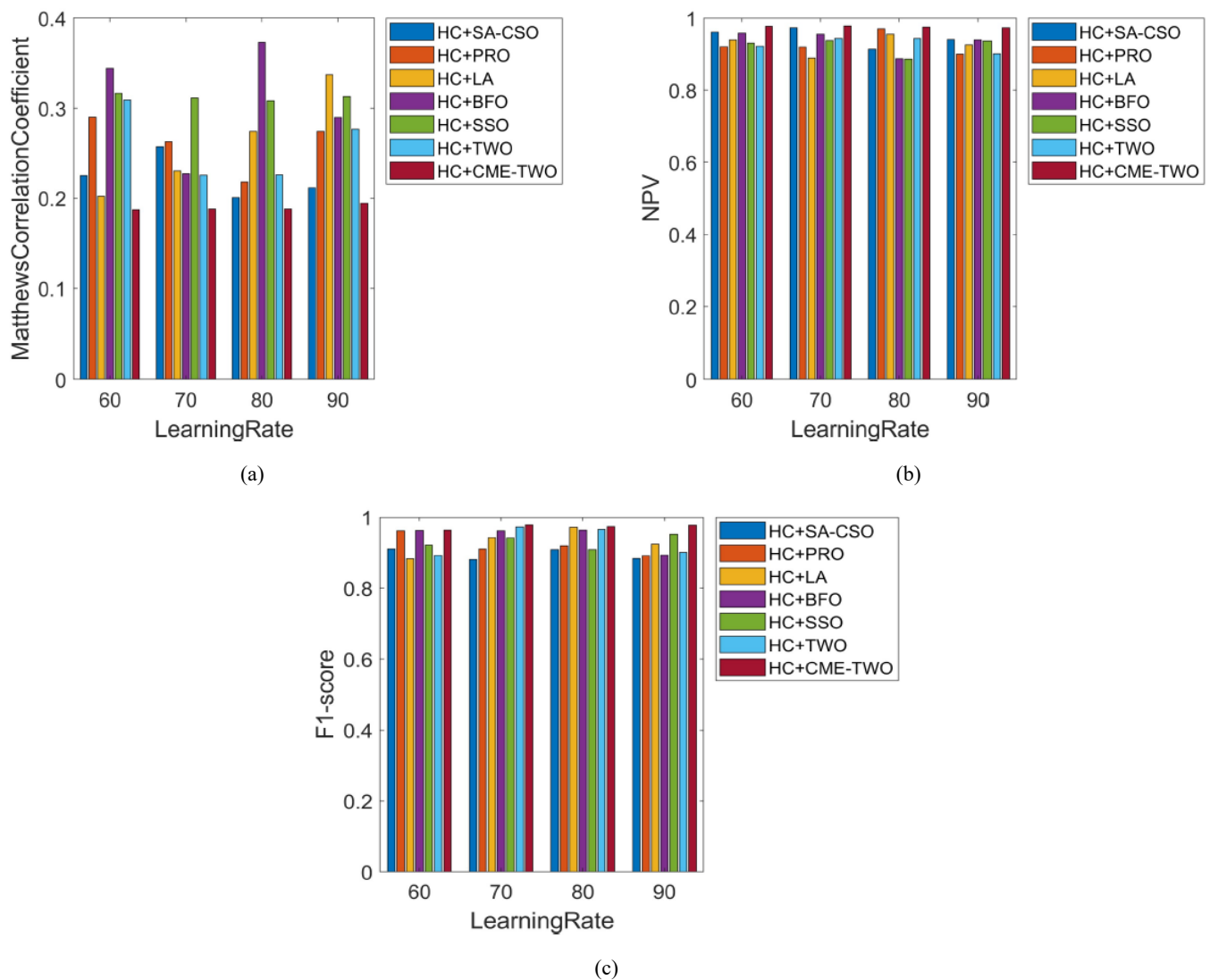

(a)

(b)

(c)

Table 3   Analysis on HC + CME-TWO model over existing classification schemes

Metrics (%)	BI-LSTM	NN	LSTM	DBN	GRU	HC + CME-TWO
			LR = 60			
NPV	0.89591	0.94337	0.89145	0.966	0.94627	0.97717
Sensitivity	0.93363	0.91056	0.9413	0.92445	0.94531	0.97425
MCC	0.2742	0.31645	0.29507	0.37159	0.27201	0.1872
Specificity	0.9295	0.97639	0.90322	0.90838	0.954	0.97775
FPR	0.19277	0.32364	0.25583	0.2569	0.31752	0.19143
F1-score	0.91884	0.88707	0.89818	0.89313	0.90908	0.96377
Precision	0.90976	0.92429	0.93887	0.90959	0.93504	0.96878
FNR	0.33115	0.3431	0.25863	0.30446	0.29584	0.18905
Accuracy	0.83849	0.87126	0.88997	0.85272	0.87248	0.95762
FDR	0.36512	0.37997	0.36378	0.20535	0.23732	0.19413
			LR = 70			
NPV	0.92172	0.94749	0.90026	0.96592	0.93856	0.97841
Precision	0.93764	0.93291	0.94181	0.92796	0.96753	0.97729
MCC	0.23877	0.27567	0.25106	0.34266	0.2697	0.18784
Accuracy	0.75255	0.87024	0.91923	0.81291	0.76342	0.95243
FPR	0.26313	0.36406	0.36877	0.30037	0.30379	0.18258
F1-score	0.95614	0.9032	0.8991	0.92844	0.8952	0.9783
Specificity	0.91467	0.92115	0.92708	0.90013	0.97593	0.97697
FNR	0.34558	0.34273	0.2553	0.21327	0.22887	0.21051
Sensitivity	0.92166	0.91861	0.9578	0.95356	0.90396	0.97747
FDR	0.26217	0.35831	0.29566	0.36244	0.38373	0.20038
			LR = 80			
Specificity	0.93904	0.95108	0.92572	0.96664	0.94349	0.97099
FDR	0.31512	0.27276	0.2095	0.35699	0.35657	0.20873
FNR	0.37281	0.21449	0.35884	0.27741	0.34242	0.1924
MCC	0.19928	0.19338	0.23962	0.33216	0.21799	0.18809
Sensitivity	0.95949	0.94476	0.93705	0.95434	0.91561	0.9724
NPV	0.88639	0.9573	0.8932	0.89393	0.9345	0.97535
Precision	0.9474	0.9274	0.91757	0.95378	0.93205	0.9698
FPR	0.21354	0.34014	0.22934	0.32114	0.19114	0.18973
Accuracy	0.89318	0.86734	0.86948	0.81183	0.74357	0.95593
F1-score	0.90654	0.95888	0.90075	0.90763	0.89085	0.97354
			LR = 90			
MCC	0.37968	0.32846	0.3206	0.32642	0.19887	0.19477
Accuracy	0.82278	0.87146	0.86258	0.7722	0.75083	0.95788
Precision	0.92963	0.9401	0.91699	0.91738	0.9415	0.97351
FPR	0.28283	0.20784	0.33902	0.29243	0.35414	0.20727
F1-score	0.93966	0.9096	0.92588	0.88758	0.95773	0.97702
FNR	0.29076	0.28555	0.35242	0.30072	0.35255	0.18895
Specificity	0.96147	0.90568	0.95449	0.90389	0.92655	0.97506
NPV	0.95986	0.91655	0.90854	0.96304	0.9213	0.97361
Sensitivity	0.93356	0.90995	0.93222	0.94652	0.96921	0.9798
FDR	0.29183	0.22929	0.2925	0.31493	0.31199	0.19354

Figure 5 Analysis on HC + CME-TWO with traditional optimisation method concerning (a) FPR (b) FNR and (c) FDR (see online version for colours)

(a)

(b)

(c)
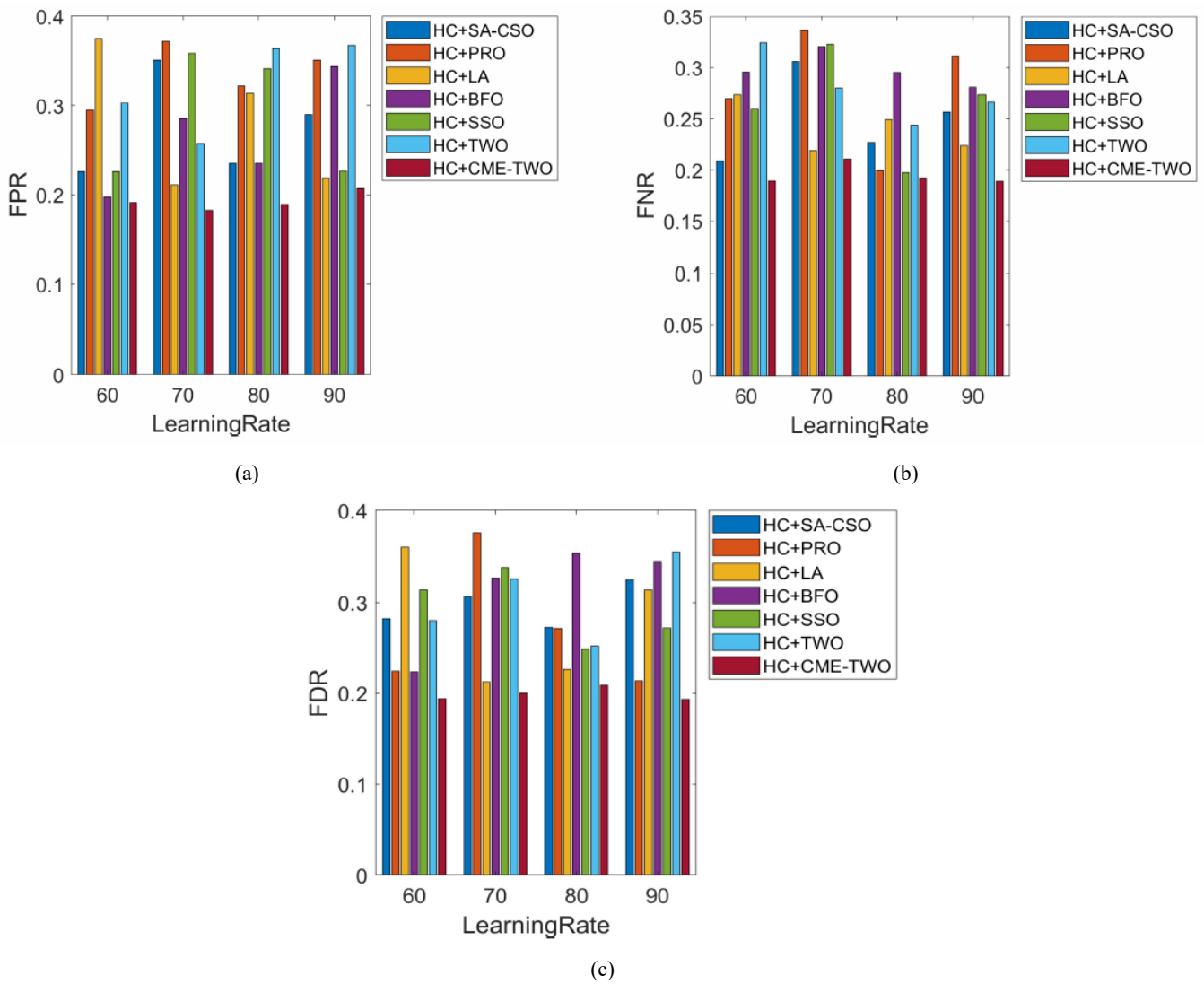
Figure 6 Convergence analysis (see online version for colours)
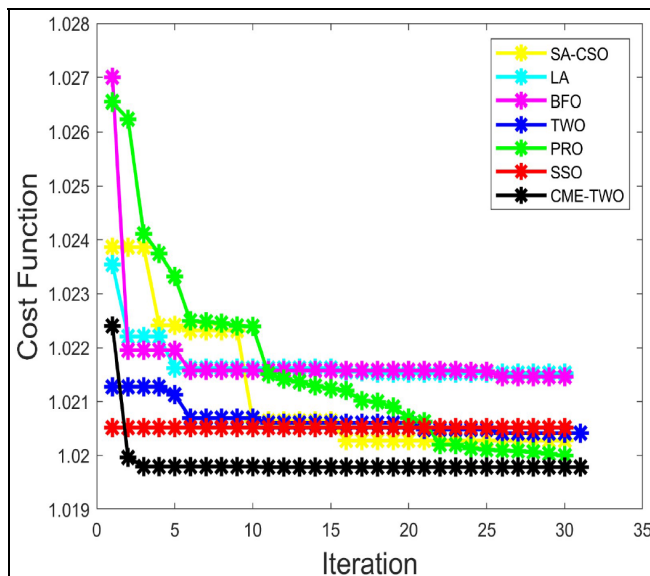
Table 4 Analysis on conventional features and proposed optimisation method

Metrics	*Proposed without optimisation*	*Proposed without feature extraction*	*Proposed with extant CNN features*	*HC + CME-TWO*
FDR	0.21256	0.33579	0.29339	0.20873
Precision	0.95585	0.95466	0.92836	0.9698
FNR	0.24485	0.3098	0.22225	0.1924
Accuracy	0.72363	0.67506	0.75939	0.95593
FPR	0.27996	0.2934	0.35911	0.18973
Sensitivity	0.93649	0.91312	0.93654	0.9724
F1-score	0.93648	0.92566	0.94518	0.97354
MCC	0.30218	0.18865	0.27651	0.18809
Specificity	0.91552	0.91837	0.93362	0.97099
NPV	0.93657	0.90057	0.91629	0.97535

Table 5   Statistical analysis of HC + CME-TWO and existing models

	Bi-LSTM	NN	LSTM	DBN	GRU	HC + SA-CSO	HC + PRO	HC + LA	HC + BFO	HC + SSO	HC + TWO	HC + CME-TWO
					Accuracy							
Mean	0.827	0.870	0.885	0.812	0.783	0.853	0.897	0.936	0.915	0.869	0.897	0.956
Best	0.753	0.867	0.863	0.772	0.744	0.837	0.844	0.924	0.892	0.858	0.862	0.952
Median	0.831	0.871	0.880	0.812	0.757	0.854	0.910	0.937	0.920	0.866	0.896	0.957
Worst	0.893	0.871	0.919	0.853	0.872	0.867	0.925	0.945	0.928	0.888	0.932	0.958
Std. dev.	0.058	0.002	0.025	0.033	0.060	0.013	0.036	0.009	0.016	0.013	0.029	0.003
					Sensitivity							
Mean	0.173	0.031	0.115	0.188	0.193	0.147	0.103	0.064	0.085	0.131	0.103	0.044
Best	0.107	0.030	0.081	0.147	0.029	0.133	0.075	0.055	0.072	0.112	0.068	0.042
Median	0.169	0.031	0.120	0.188	0.243	0.146	0.090	0.063	0.080	0.134	0.104	0.043
Worst	0.247	0.034	0.137	0.228	0.256	0.163	0.156	0.076	0.108	0.142	0.138	0.048
Std. dev.	0.058	0.002	0.025	0.033	0.110	0.013	0.036	0.009	0.016	0.013	0.029	0.003
					Specificity							
Best	0.922	0.910	0.932	0.924	0.904	0.914	0.920	0.904	0.920	0.919	0.914	0.972
Mean	0.937	0.921	0.942	0.945	0.934	0.930	0.943	0.929	0.944	0.946	0.942	0.976
Median	0.934	0.915	0.939	0.950	0.930	0.925	0.945	0.925	0.940	0.947	0.945	0.976
Worst	0.959	0.945	0.958	0.954	0.969	0.955	0.962	0.962	0.976	0.971	0.963	0.980
Std. dev.	0.016	0.016	0.011	0.014	0.029	0.018	0.018	0.027	0.023	0.022	0.022	0.003
					Precision							
Best	0.915	0.906	0.903	0.900	0.927	0.919	0.900	0.904	0.902	0.911	0.929	0.971
Worst	0.961	0.976	0.954	0.967	0.976	0.948	0.928	0.968	0.960	0.941	0.972	0.978
Mean	0.936	0.939	0.928	0.920	0.950	0.936	0.914	0.940	0.923	0.924	0.949	0.975
Median	0.934	0.936	0.926	0.906	0.949	0.938	0.914	0.944	0.916	0.922	0.947	0.976
Std. dev.	0.020	0.031	0.021	0.031	0.021	0.013	0.015	0.027	0.026	0.013	0.020	0.003
					FPR							
Best	0.910	0.924	0.917	0.910	0.932	0.916	0.909	0.901	0.913	0.901	0.904	0.969
Worst	0.947	0.940	0.942	0.954	0.968	0.967	0.943	0.959	0.967	0.968	0.947	0.977
Mean	0.931	0.931	0.929	0.927	0.944	0.933	0.925	0.927	0.941	0.944	0.924	0.972
Median	0.934	0.930	0.928	0.923	0.938	0.924	0.924	0.925	0.941	0.954	0.923	0.972
Std. dev.	0.016	0.007	0.013	0.019	0.016	0.023	0.014	0.031	0.024	0.031	0.017	0.004
					F1-score							
Best	0.193	0.208	0.229	0.257	0.191	0.211	0.295	0.226	0.198	0.226	0.257	0.183
Worst	0.283	0.364	0.369	0.321	0.354	0.375	0.372	0.351	0.344	0.358	0.367	0.207
Mean	0.238	0.309	0.298	0.293	0.292	0.280	0.335	0.276	0.266	0.288	0.323	0.193
Median	0.238	0.332	0.297	0.296	0.311	0.267	0.336	0.263	0.260	0.284	0.333	0.191
Std. dev.	0.042	0.069	0.066	0.027	0.070	0.079	0.033	0.057	0.063	0.072	0.053	0.010
					MCC							
Mean	0.930	0.915	0.906	0.904	0.913	0.930	0.921	0.896	0.945	0.931	0.933	0.973
Best	0.907	0.887	0.898	0.888	0.891	0.882	0.892	0.881	0.893	0.909	0.892	0.964
Median	0.929	0.906	0.900	0.900	0.902	0.933	0.915	0.896	0.962	0.932	0.933	0.975
Worst	0.956	0.959	0.926	0.928	0.958	0.972	0.961	0.910	0.964	0.952	0.972	0.978
Std. dev.	0.022	0.031	0.013	0.018	0.031	0.037	0.029	0.016	0.035	0.020	0.042	0.007

Table 5   Statistical analysis of HC + CME-TWO and existing models (continued)

	Bi-LSTM	NN	LSTM	DBN	GRU	HC + SA-CSO	HC + PRO	HC + LA	HC + BFO	HC + SSO	HC + TWO	HC + CME-TWO
						FNR						
Mean	0.273	0.278	0.277	0.343	0.240	0.261	0.261	0.224	0.309	0.312	0.259	0.189
Best	0.199	0.193	0.240	0.326	0.199	0.202	0.218	0.201	0.227	0.308	0.225	0.187
Median	0.256	0.296	0.273	0.337	0.244	0.252	0.268	0.218	0.317	0.312	0.251	0.188
Worst	0.380	0.328	0.321	0.372	0.272	0.337	0.290	0.257	0.373	0.317	0.309	0.195
Std. dev.	0.077	0.061	0.038	0.020	0.037	0.059	0.031	0.024	0.064	0.004	0.041	0.004
						NPV						
Mean	0.013	0.130	0.057	0.009	0.016	0.636	0.726	0.660	0.781	0.652	0.646	0.901
Best	0.000	0.101	0.006	0.002	0.003	0.566	0.584	0.121	0.712	0.622	0.429	0.893
Median	0.015	0.123	0.070	0.010	0.014	0.639	0.760	0.827	0.787	0.641	0.695	0.903
Worst	0.021	0.173	0.081	0.015	0.032	0.700	0.799	0.865	0.838	0.701	0.764	0.905
Std. dev.	0.010	0.031	0.035	0.006	0.013	0.065	0.097	0.360	0.052	0.035	0.148	0.006
						FDR						
Median	0.338	0.314	0.306	0.289	0.319	0.237	0.291	0.242	0.295	0.267	0.273	0.191
Best	0.291	0.214	0.255	0.213	0.229	0.219	0.200	0.209	0.281	0.198	0.244	0.189
Mean	0.335	0.296	0.306	0.274	0.305	0.241	0.279	0.250	0.298	0.263	0.279	0.195
Worst	0.373	0.343	0.359	0.304	0.353	0.274	0.336	0.306	0.320	0.323	0.324	0.211
Std. dev.	0.034	0.061	0.057	0.042	0.056	0.025	0.060	0.042	0.016	0.052	0.034	0.010

6.5 Feature analysis

Table 4 depicts the analysis of HC + CME-TWO scheme over adopted model without optimisation, adopted model without feature extraction and adopted model with extant CNN features. From the results, the HC + CME-TWO have accomplished the better result than the adopted model without optimisation, adopted model without feature extraction and adopted model with extant CNN features. Moreover, the HC + CME-TWO method without feature extraction has revealed comparatively worst outputs than developed model without optimisation and developed model with extant CNN features. This demonstrates the enhancement of the feature extracting concept and proposed optimisation concept in the proposed work.

6.6 Statistical analysis

The metaheuristic schemes are stochastic and to prove better evaluation results, every model is examined numerous times to accomplish objective function. Table 5 symbolises the statistical analysis of the proposed HC + CME-TWO method with extant models regarding accuracy. On observing the outcomes, for every scenario, the developed HC + CME-TWO scheme has attained high values for positive measures and low values for negative measures. The mean outcomes of suggested HC + CME-TWO approach holds (0.956) superior results than the traditional schemes which is 13.49%, 9.00%, 7.43%, 15.06%, 18.10%, 10.77%, 6.17%, 2.09%, 4.29%, 9.10% and 6.17% superior than BI-LSTM, NN, LSTM, DBN, GRU, HC + SA-CSO, HC + PRO, HC + LA,

HC + BFO, HC + SSO and HC + TWO, respectively. Moreover, the proposed method for median holds (0.957) HC + CME-TWO method, which is 13.17%, 8.99%, 8.05%, 15.15%, 20.90%, 10.76%, 4.91%, 2.09%, 3.87%, 9.51%, 6.37% higher than the traditional models like BI-LSTM, NN, LSTM, DBN, GRU, HC + SA-CSO, HC + PRO, HC + LA, HC + BFO, HC + SSO and HC + TWO, respectively. Thus, the improvement of the adopted scheme was proven.

7 Conclusions

This research work introduces a novel model for identifying food ingredients. These features were then classified via hybrid classifiers that included NN and LSTM models. In particular, the weights of NN and LSTM were tuned in an optimal way using the CME-TWO model. Further, the performance of proposed model was evaluated over existing models like HC + SA-CSO, HC + PRO, HC + LA, HC + BFO, HC + SSO and HC + TWO concerning various metrics. From the, the developed HC + CME-TWO scheme has gained suitable values (high outputs for positive measures and low outputs for negative metrics) for every scenario. The mean outcomes of suggested HC + CME-TWO model has accomplished better outputs of (0.956) superior results than the traditional schemes which is 13.49%, 9.00%, 7.43%, 15.06%, 18.10%, 10.77%, 6.17%, 2.09%, 4.29%, 9.10% and 6.17% superior than BI-LSTM, NN, LSTM, DBN, GRU, HC + SA-CSO, HC + PRO, HC + LA, HC + BFO, HC + SSO and HC + TWO. Further, the HC + CME-TWO have accomplished the better values

than the adopted model without optimisation, the developed model without feature extraction and proposed model with extant CNN features. The proposed method is useful in various applications, such as food management, and so on. The future concern of this research would be the plan of developing effective time analysis for improving effectiveness of food ingredient recognition.

References

Aguiar, L.K., Martinez, D.C. and Caleman, S.M.Q. (2018) 'Consumer awareness of palm oil as an ingredient in food and non-food products', *Journal of Food Products Marketing*, Vol. 24, No. 3, pp.297–310, DOI: 10.1080/10454446.2017.1266559.

Ambrosini, G.L., Hurworth, M., Giglia, R. et al. (2018) 'Feasibility of a commercial smartphone application for dietary assessment in epidemiological research and comparison with 24-h dietary recalls', *Nutr. J.*, Vol. 17, No. 5 [online] https://doi.org/10.1186/s12937-018-0315-4.

Dehghani, M. and Trojovský, P. (2021) 'Teamwork optimization algorithm: a new optimization approach for function minimization/maximization', *Sensors*, Vol. 21, p.4567 [online] https://doi.org/10.3390/s21134567.

Emmanuel, W.R.S. and Minija, S.J. (2018) 'Fuzzy clustering and whale-based neural network to food recognition and calorie estimation for daily dietary assessment', *Sādhanā*, Vol. 43, No. 78 [online] https://doi.org/10.1007/s12046-018-0865-3.

Fernandes, A.R., Mortimer, D., Rose, M. and Panton, S. (2019) 'Recently listed Stockholm convention POPs: analytical methodology, occurrence in food and dietary exposure', *Science of the Total Environment*, first available: 3 May, 15 August, Vol. 678, pp.793–800.

George, A. and Rajakumar, B.R. (2013) 'APOGA: an adaptive population pool size based genetic algorithm', *AASRI Procedia – 2013 AASRI Conference on Intelligent Systems and Control (ISC 2013)*, Vol. 4, pp.288–296, DOI [online] https://doi.org/10.1016/j.aasri.2013.10.043.

Gu, J., Wang, Z., Kuen, J., Ma, L., Shahroudy, A., Shuai, B., Liu, T., Wang, X., Wang, G., Cai, J. and Chen, T. (2018) 'Recent advances in convolutional neural networks', *Pattern Recognition*, Vol. 77, pp.354–377.

Guo, A. and Yang, T. (2016) 'Research and improvement of feature words weight based on TFIDF algorithm', *2016 IEEE Information Technology, Networking, Electronic and Automation Control Conference*, DOI: 10.1109/itnec.2016.7560393.

Hafiz, R., Haque, M.R., Rakshit, A. and Uddin, M.S. (2020) 'Image-based soft drink type classification and dietary assessment system using deep convolutional neural network with transfer learning', *Journal of King Saud University – Computer and Information Sciences*, 9 September, No. 5, pp.1775–1784.

Hellmann, S.L., Ripp, F., Sven-Ernö, B., Schmidt, B., Köppel, R. et al. (2020) 'Identification and quantification of meat product ingredients by whole-genome metagenomics (All-Food-Seq)', *European Food Research and Technology, Zeitschrift für Lebensmittel-Untersuchung und -Forschung. A*, January, Vol. 246, No. 1, pp.193–200, Heidelberg, DOI: 10.1007/s00217-019-03404-y.

Iqbal, S.Z., Mumtaz, A., Mahmood, Z. and Pervaiz, W. (2021) 'Assessment of aflatoxins and ochratoxin a in chili sauce samples and estimation of dietary intake', *Food Control*, first available: 14 September 2020, March, Vol. 121, pp.1–7, Article 107621.

Jadhav, A.N. and Gomathi, N. (2019) 'DIGWO: hybridization of dragonfly algorithm with improved grey wolf optimization algorithm for data clustering', *Multimedia Research*, Vol. 2, No. 3, pp.1–11.

Jiang, L., Qiu, B., Liu, X., Huang, C. and Lin, K. (2020) 'DeepFood: food image analysis and dietary assessment via deep model', *IEEE Access*, Vol. 8, pp.47477–47489, DOI: 10.1109/ACCESS.2020.2973625.

Kim, D., Seo, D., Cho, S. and Kang, P. (2018) 'Multi-co-training for document classification using various document representations: TF–IDF, LDA, and Doc2Vec', *Information Sciences*, DOI: 10.1016/j.ins.2018.10.006.

Kuo, J-H., Tsuei, H-W., Jia, Z-L., Lin, C-Y., Chang, Y-H., Chen, B-L., Kuan, J., Lin, H-Y., Chiueh, L-C., Shih, D.Y-C., Cheng, H-F. (2018) 'Identification of ingredient in mullet roe products by the real-time PCR method', *Food Analytical Methods*, Vol. 11, No. 4, pp.992–1000.

Li, H., Gao, S., Yang, M. and Cai, Z. (2020) 'Dietary exposure and risk assessment of short-chain chlorinated paraffins in supermarket fresh products in Jinan, China', *Chemosphere*, first available: 23 November 2019, April, Vol. 244, pp.1–6, Article 125393.

Liu, C. et al. (2018) 'A new deep learning-based food recognition system for dietary assessment on an edge computing service infrastructure', *IEEE Transactions on Services Computing*, 1 March–April, Vol. 11, No. 2, pp.249–261, DOI: 10.1109/TSC.2017.2662008.

Liu, L., Han, J., Xu, X. et al. (2020) 'Dietary exposure assessment of cadmium, arsenic, and lead in market rice from Sri Lanka', *Environ. Sci. Pollut. Res.* [online] https://doi.org/10.1007/s11356-020-10209-0.

Liu, Y-C., Chen, C-H., Lee, C-W. and Chiu, S.Y-H. (2016) 'Design and usability evaluation of user-centered and visual-based aids for dietary food measurement on mobile devices in a randomized controlled trial', *Journal of Biomedical Informatics*, first available: 5 October, December, Vol. 64, pp.122–130.

Lo, F.P-W., Sun, Y., Qiu, J. and Lo, B.P.L. (2020) 'Point2Volume: a vision-based dietary assessment approach using view synthesis', *IEEE Transactions on Industrial Informatics*, January, Vol. 16, No. 1, pp.577–586, DOI: 10.1109/TII.2019.2942831.

Macheka, L.R., Olowoyo, J.O., Mugivhisa, L.L. and Abafe, O.A. (2021) 'Determination and assessment of human dietary intake of per and polyfluoroalkyl substances in retail dairy milk and infant formula from South Africa', *Science of the Total Environment*, first available: 2 October 2020, 10 February, Vol. 755, pp.1–8, Part 2, Article 142697.

Madival, S.A. and Jawaligi, S.S. (2022) 'Dietary assessment framework using improved K-means clustering and optimisation assisted CNN', *Computer Methods in Biomechanics and Biomedical Engineering: Imaging & Visualization*, pp.1–14.

Mohan, Y., Chee, S.S., Xin, D.K.P. and Foong, L.P. (2016) 'Artificial neural network for classification of depressive and normal in EEG', *2016 IEEE EMBS Conference on Biomedical Engineering and Sciences (IECBES)*.

Navruz-Varlı, S., Köse, S., Tatar, T. et al. (2018) 'Assessment of dietary calcium intake of university students: a pilot study in Turkey', *Arch. Osteoporos.*, Vol. 13, p.36 [online] https://doi.org/10.1007/s11657-018-0447-3.

Nipanikar, S.I. and Hima Deepthi, V. (2019) 'Enhanced whale optimization algorithm and wavelet transform for image steganography', *Multimedia Research*, Vol. 2, No. 3, pp.23–32.

Pang, N., Fan, X., Fantke, P. and Hu, J. (2020) 'Dynamics and dietary risk assessment of thiamethoxam in wheat, lettuce and tomato using field experiments and computational simulation', *Environmental Pollution*, first available: 20 September 2019, January, Vol. 256, Article 113285.

Pearce, A.L., Adise, S., Roberts, N.J. and Keller, K.L. (2020) 'Individual differences in the influence of taste and health impact successful dietary self-control: a mouse tracking food choice study in children', *Physiology & Behavior*, first available: 4 June, September, Vol. 223, Article 112990.

Rajakumar, B.R. (2013a) 'Static and adaptive mutation techniques for genetic algorithm: a systematic comparative analysis', *International Journal of Computational Science and Engineering*, Vol. 8, No. 2, pp.180–193, DOI: 10.1504/IJCSE.2013.053087.

Rajakumar, B.R. (2013b) 'Impact of static and adaptive mutation techniques on genetic algorithm', *International Journal of Hybrid Intelligent Systems*, Vol. 10, No. 1, pp.11–22, DOI: 10.3233/HIS-120161.

Rajakumar, B.R. and George, A. (2012) 'A new adaptive mutation technique for genetic algorithm', in *Proceedings of IEEE International Conference on Computational Intelligence and Computing Research (ICCIC)*, Coimbatore, India, 18–20 December, pp.1–7, DOI: 10.1109/ICCIC.2012.6510293.

Sadashiv Halbhavi, B., Kodad, S.F., Ambekar, S.K. and Manjunath, D. (2019) 'Enhanced invasive weed optimization algorithm with chaos theory for weightage based combined economic emission dispatch', *Journal of Computational Mechanics, Power System and Control*, Vol. 2, No. 3, pp.19–27.

Santosh Kumar, B.P. and Venkata Ramanaiah, K. (2019) 'An efficient hybrid optimization algorithm for image compression', *Multimedia Research*, Vol. 2, No. 4, pp.1–11.

SIFT Feature [online] https://medium.com/data-breach/introduction-to-sift-scaleinvariant-feature-transform-65d7f3a72d40 (accessed 17 2021).

Sreenivasu, S.V.N., Gomathi, S., Kumar, M.J., Prathap, L., Madduri, A., Almutairi, K.M.A., Alonazi, W.B., Kali, D. and Jayadhas, S.A. (2022) 'Dense convolutional neural network for detection of cancer from CT images', *BioMed Research International*, Vol. 2022, 8pp, Article ID: 1293548.

Swamy, S.M., Rajakumar, B.R. and Valarmathi, I.R. (2013) 'Design of hybrid wind and photovoltaic power system using opposition-based genetic algorithm with Cauchy mutation', *IET Chennai Fourth International Conference on Sustainable Energy and Intelligent Systems (SEISCON 2013)*, Chennai, India, December, DOI: 10.1049/ic.2013.0361.

Thulasi, P.K. (2017) 'Sentiment analysis in Malayalam', *International Journal of Advanced Research in Computer and Communication Engineering*.

Vinusha, S. (2019) 'Secret image sharing and steganography using Haar wavelet transform', *Multimedia Research*, Vol. 2, No. 2, pp.28–34.

Wagh, M.B. and Gomathi, N. (2019) 'Improved GWO-CS algorithm-based optimal routing strategy in VANET', *Journal of Networking and Communication Systems*, Vol. 2, No. 1, pp.34–42.

Wahls, T., Rubenstein, L., Hall, M. and Snetselaar, L. (2014) 'Assessment of dietary adequacy for important brain micronutrients in patients presenting to a traumatic brain injury clinic for evaluation', *Nutritional Neuroscience*, Vol. 17, No. 6, pp.252–259, DOI: 10.1179/1476830513Y.0000000088.

Wald, J.P., Asare, E., Nakua, E.K. and Biesalski, H.K. (2019) 'Validation of a computer-based analysis tool for real-time dietary assessment within a Ghanaian region', *NFS Journal*, first available: 25 June, September, Vol. 16, pp.15–25.

Wang, Y., He, Y., Boushey, C.J. et al. (2018a) 'Context based image analysis with application in dietary assessment and evaluation', *Multimed. Tools Appl.*, Vol. 77, pp.19769–19794 [online] https://doi.org/10.1007/s11042-017-5346-x.

Wang, S., Zhang, Q., Yu, Y. and Hu, D. (2018b) 'Residues, dissipation kinetics, and dietary intake risk assessment of two fungicides in grape and soil', *Regulatory Toxicology and Pharmacology*, first available: 22 October, December, Vol. 100, pp.72–79.

Zhao, Z., Sun, R., Su, Y. and Liu, X. (2020a) 'Fate, residues and dietary risk assessment of the fungicides epoxiconazole and pyraclostrobin in wheat in twelve different regions, China', *Ecotoxicology and Environmental Safety*, first available: 7 September, January 2021, Vol. 207, Article 1112361.

Zhao, L., Li, S., Hua, M.Z., Liu, J., Zhang, H., Hu, Y., Chen, Y., Lu, X. and Zheng, W. (2020b) 'Development of a species-specific PCR coupled with lateral flow immunoassay for the identification of goose ingredient in foods', *Food Control*, Vol. 114, p.107240, ISSN: 0956-7135.

Zheng, X., Pu, P., Ding, B., Bo, W., Qin, D. and Liang, G. (2021) 'Identification of the functional food ingredients with antithrombotic properties via virtual screen and experimental studies', *Food Chem.*, 15 November, Epub: May 29, Vol. 362, p.130237, PMID: 34091163, DOI: 10.1016/j.foodchem.2021.130237.

Zhou, X., Lin, J., Zhang, Z., Shao, Z. and Liu, H. (2019) 'Improved itracker combined with bidirectional long short-term memory for 3D gaze estimation using appearance cues', *Neuro Computing*, online: 20 October, in press.

Websites

http://www.ub.edu/cvub/recipes5k/.

https://neptune.ai/blog/gan-loss-functions.

https://nextjournal.com/jbowles/n-gram-models-part-1#:~:text=An%20n%2Dgram%20model%20is,rich%20pattern%20discovery%20in%20text.&text=In%20other%20words%2C%20it%20tries,or%20words%20near%20each%20other.

Nomenclature

Abbreviation	Description
BFO	Butterfly optimisation
BOW	Bag of words
CIMI	Calculator of inadequate micronutrient intake
CME-TWO	Chebyshev map evaluated TWO
CNN	Convolutional neural network
CSW-WLFC	Cauchy, generalised T-student, and wavelet kernel based Wu and Li index fuzzy clustering
DBN	Deep belief network
DCNN	Deep CNN
FDR	False discovery rate
FNR	False negative rate
FPR	False positive rate
GRUs	Gated recurrent units
LA	Lion algorithm
LFI	Lateral flow immunoassay
LR	Learning rate
LSTM	Long short-term memory
MCC	Matthews correlation coefficient
NN	Neural network
NPV	Negative predictive value
PCR	Polymerase chain reaction
PRO	Poor and rich optimisation
SA-CSO	Self-adaptive cat swarm optimisation
SIFT	Scale invariant – inverse document frequency
SSO	Shark smell optimisation
TF-IDF	Term frequency inverse document frequency
TWO	Team work optimisation
WLM	Whale-Levenberg Marquardt